

The Magnus effect and the American football

Christian Guzman, Cody Brownell & Eric M. Kommer

Sports Engineering

ISSN 1369-7072

Volume 19

Number 1

Sports Eng (2016) 19:13-20

DOI 10.1007/s12283-015-0184-4



Your article is protected by copyright and all rights are held exclusively by International Sports Engineering Association. This e-offprint is for personal use only and shall not be self-archived in electronic repositories. If you wish to self-archive your article, please use the accepted manuscript version for posting on your own website. You may further deposit the accepted manuscript version in any repository, provided it is only made publicly available 12 months after official publication or later and provided acknowledgement is given to the original source of publication and a link is inserted to the published article on Springer's website. The link must be accompanied by the following text: "The final publication is available at link.springer.com".

The Magnus effect and the American football

Christian Guzman¹ · Cody Brownell² · Eric M. Kommer¹

Published online: 25 September 2015
© International Sports Engineering Association 2015

Abstract The aerodynamics of an American NFL football during an end over end kick were investigated utilizing a custom rotating apparatus and large-scale wind tunnel. Non-rotating lift and drag coefficients were measured and agree well with previous data from other athletic balls and a smooth sphere. The rotation effect on an American football increased both the lift and drag coefficients more dramatically than what has been seen with symmetrical objects over a wide range of rotational rates. The results from this study can be used to more accurately predict the flight trajectory of an end over end kick, and help optimize the balance between kick velocity and rotational speed for a given kicker's leg strength.

Keywords Aerodynamics · American football · Magnus effect · Rotational velocity · Kick · Drag

1 Background

The curvature of trajectory on a spinning ball has been observed and commented on as early as 1671 by Sir Issac Newton [1] and is commonly referred to the Magnus (or sometimes Robins) effect, after Dr. Heinrich Magnus, who qualitatively described the phenomenon in 1928 [2]. Tennis slices, baseball curveballs, and golf hooks are all outcomes of the Magnus effect in which a lateral force is imparted on

a symmetric body due only to the rotation of the object. This lateral force is more commonly described as a lift force, and is due to the rotation of the object dragging the fluid boundary layer in the direction of rotation, modifying the pressure distribution and imparting a net force on the object.

The Magnus effect has been extensively studied over the last century by researchers with objects of many shapes and sizes. Lift and drag coefficients of sports balls with rotation have been measured via a variety of methods. In baseball, the laces on the ball allow the Magnus effect to be amplified greatly, leading to the ability of pitchers to throw a variety of pitches, normally termed breaking balls, such as a slider, curveball, or sinker [3–5]. The curvature of soccer corner kicks has been evaluated using high speed visualization to determine the effect of rotation speed [6, 7]. Wind tunnel testing to determine the lift and drag coefficients of non-rotating soccer balls has been performed with full scale balls [8–11]. Investigation into Australian rules football and rugby balls is also found in the literature [12].

With respect to American footballs, wind tunnel testing has been performed to determine drag coefficients of non-rotating balls [13]. Scale testing has been performed on footballs spinning along the longitudinal axis, as in a spiral throw [14]. A number of purely kinematic studies on American footballs have been published which attempt to quantify either the stabilizing effect of a spiral or the oscillation of the drag and lift force due to rotation [15–18]. Simulations and/or computations of ball flight have often used lift and drag coefficients calculated on a non-rotating ball. Past research on smooth spheres shows that as rotational speed increases, lift and drag coefficients can vary drastically.

✉ Eric M. Kommer
kommer@cua.edu

¹ The Catholic University of America, 620 Michigan Ave NE, Washington, DC 20064, USA

² United States Naval Academy, 590 Holloway Rd, Annapolis, MD 21402, USA

Nowhere in the literature has the Magnus effect been quantified for an American football with end-over-end rotation. The football is especially interesting because during end over end rotation, such as seen during kickoffs, the ball's front projected area changes dramatically and due to the presence of the laces it is asymmetric. Surface roughness and seams also add to the complexities of the flow, so that Magnus effect predictions extrapolated from smooth sphere data are not expected to be accurate.

Accurate predictions of the lift and drag on a football with respect to velocity and rotational speed can help predict the actual trajectory of the kick and help optimize the best rotation speed for a given kick. The aims of this work are to accurately quantify the effects of rotation on the uniquely shaped football as a means for researchers, trainers, and athletes to better understand the physics of football flight.

2 Theory

To accurately predict the trajectory of ball in flight, the initial position and velocity must be known to solve the kinematic equations. From Newton's second law of motion in vector form,

$$\Sigma \bar{F} = m \frac{\partial^2 \bar{x}}{\partial t^2}, \quad (1)$$

where \bar{F} is the force vector acting on the body, m is the mass of the ball, t is time, and \bar{x} is the position vector. The forces acting on the ball when in flight other than due to gravity are aerodynamic drag and lift where

$$F_L = C_L \frac{1}{2} \rho A V^2 \quad (2)$$

$$F_D = C_D \frac{1}{2} \rho A V^2, \quad (3)$$

where C_L and C_D are the lift and drag coefficients, ρ is the fluid density, and V is the velocity of the bulk fluid moving past the object. The area, A , is calculated based on the frontal projected area of the ball normal to the direction of fluid flow.

If the lift and drag coefficients are known, the solution to the ball trajectory becomes a second order non-linear differential equation that can be easily solved numerically. For most objects, the lift and drag coefficients are constant over a wide range of velocities, as long as the fundamental flow structure does not change. In most cases the flow through air is fully turbulent. For rotating bodies, a non-dimensional rotational velocity, α , is introduced:

$$\alpha = \frac{\omega D}{2V}, \quad (4)$$

where ω is the rotational velocity in radians per second, and D is the diameter. For non-symmetrical shapes, the diameter can be chosen as any appropriate length scale. In this study, the diameter is chosen to be the length of the football along the long axis. This non-dimensional velocity reaches unity when the mean flow field velocity is equal to the linear velocity of the spinning surface. At small values of α , the Magnus effect vanishes for symmetric objects. In general, as α increases, both the lift and drag coefficients increase to some limiting value. The relative magnitudes of inertial to viscous forces subjected on the object due to the flow field are represented as the Reynolds number:

$$Re = \frac{VD\rho}{\mu}, \quad (5)$$

where μ is the dynamic viscosity of the fluid in the flow field. In general, the lift and drag coefficients of an object are independent of flow velocity and Reynolds number above a critical value of the Reynolds number that ensures wholly turbulent flow over the object. Research has shown that the Magnus effect forces often do depend upon Reynolds number but not to a large degree [19].

3 Experimental apparatus

A full-sized National Football League official football was rotated about its transverse axis via an aluminum support structure and steel axle. The 6.35-mm-diameter steel axle was isolated via ball bearings and coupled to a NMEA 14 sized bipolar stepper motor. Coupling between the steel axles and the ball was accomplished using ground down T-nuts threaded onto the end of the axles. The aluminum structure made of 6.35-mm-thick 6061 alloy was assembled using threaded fasteners. The completed structure, shown in Fig. 1, was designed to minimize the blockage area in the wind tunnel to prevent accelerating the flow at the test section. All parts of the structure, except where the axles intersect the ball, were distant from the boundary layer on the ball to prevent affecting the flow field.

The AeroLab Eiffel open circuit wind tunnel in the US Naval Academy's aerospace engineering laboratory was used to conduct the testing on the apparatus. The Eiffel wind tunnel is capable of velocities up to 112 m/s and is powered by a 185 kW three-phase fan and variable frequency drive. The lift and drag forces are measured using a pyramidal 6 axis force balance with an accuracy of 0.25 % of the full scale. This equates to a rated precision of 5 N for lift and 1.3 N for the drag force. Measurements below the precision of the balance are possible but may not be accurate. Data acquisition was accomplished utilizing a desktop computer and a National Instruments NI SCXI-1314 analog to digital conversion module. This acquisition

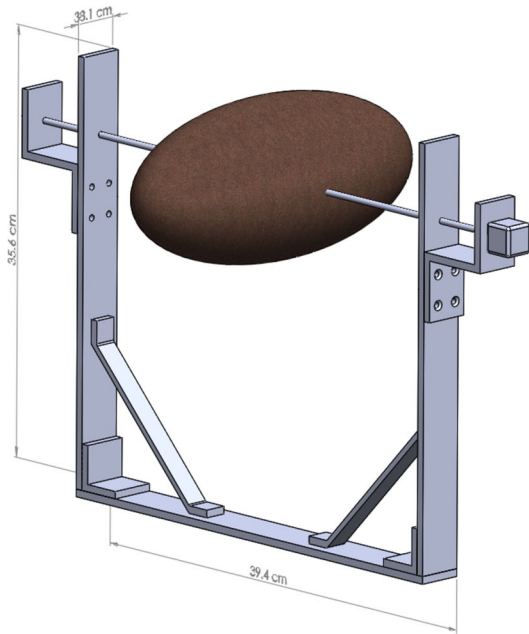


Fig. 1 Experimental apparatus

system allowed sampling at 12 ms intervals of all force transducers in the pyramidal balance. Wind tunnel velocity was determined three ways: a pitot-static tube and water manometer immediately downstream of the apparatus, a dynamic pressure gage at the laminar flow element in the entrance to the wind tunnel, and an Extech Model HD350 anemometer inserted into the test section of the tunnel.

Rotational velocity was controlled by driving the stepper motor with a signal generator via a motor driver circuit. The rotational speed of the ball was therefore directly proportional to the frequency of pulses from the signal generator assuming no pole slippage. A Shimpo model DT-205L laser tachometer was used to verify the rotational speed prior to each data collection run.

Each set of data was taken at constant wind tunnel velocity and therefore constant Reynolds number. The rotational speed of the ball was increased between 45 and 375 RPM. At some wind velocities, the low and high end of the RPM range was not possible due to inadequate motor torque or excessive apparatus vibration. Additional datasets were taken with the apparatus without rotation as well as ball rotation without wind velocity. Finally, the bare rig, without football installed, was used to determine the drag and lift effects introduced into the experiment not due to the football. Rotational and wind velocities were chosen with the aim to span the entire range of conditions normally seen during kickoffs and are summarized in Table 1. Based on data by Watts, the maximum initial velocity of a kick may exceed 20 m/s with rotational velocity not exceeding 300 RPM [14].



Table 1 Summary of experimental parameters

Parameter	Value or range	Units
Air velocity, V	4–20	m/s
Reynolds number, Re	8×10^4 to 4×10^5	–
Rotational velocity, ω	0–375	RPM
Air density, ρ	1.21	kg/m ³
Frontal area, A	0.0365	m ²
characteristic length, D	0.29	m

4 Non-rotational lift and drag results

Forty datasets were taken without rotation of the football to both quantify the component of lift and drag due to the apparatus itself, and to determine the coefficients to compare to existing research. Figure 2 shows the lift and drag coefficients of the bare rig over a range of Reynolds numbers. From this figure, it can be seen that the lift and drag of the rig are constant over this range of Reynolds numbers, and therefore can be used to correct the measurements taken with the football in place. This correction is accomplished by simply subtracting the drag or lift force due to the rig from the total.

Next, the drag coefficient for the football when positioned with the laces up, laces down, and laces forward was measured over the same range of Reynolds numbers. This type of measurement has been performed by Watts [14], and Fig. 3 shows the experimental data from this study with long axis of the ball parallel to the flow, along with

Fig. 2 Bare rig lift and drag coefficients

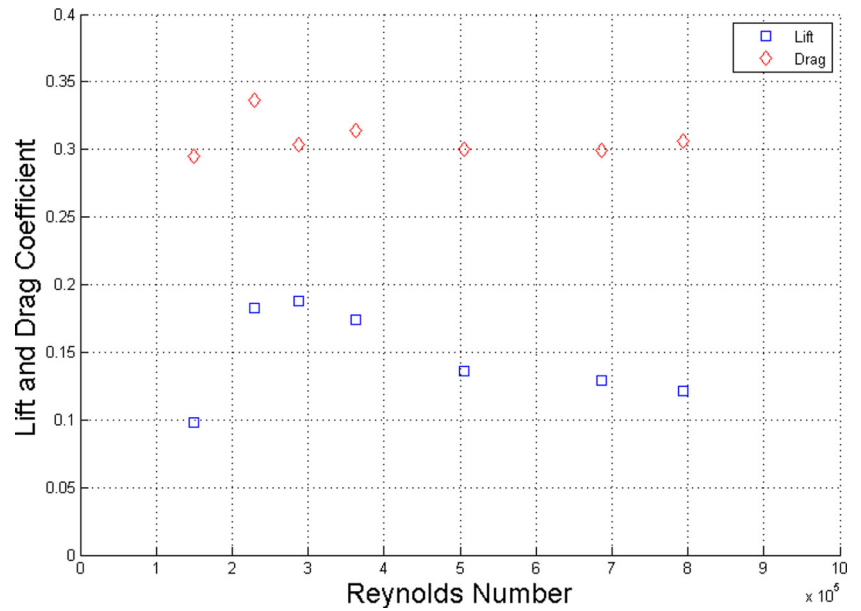
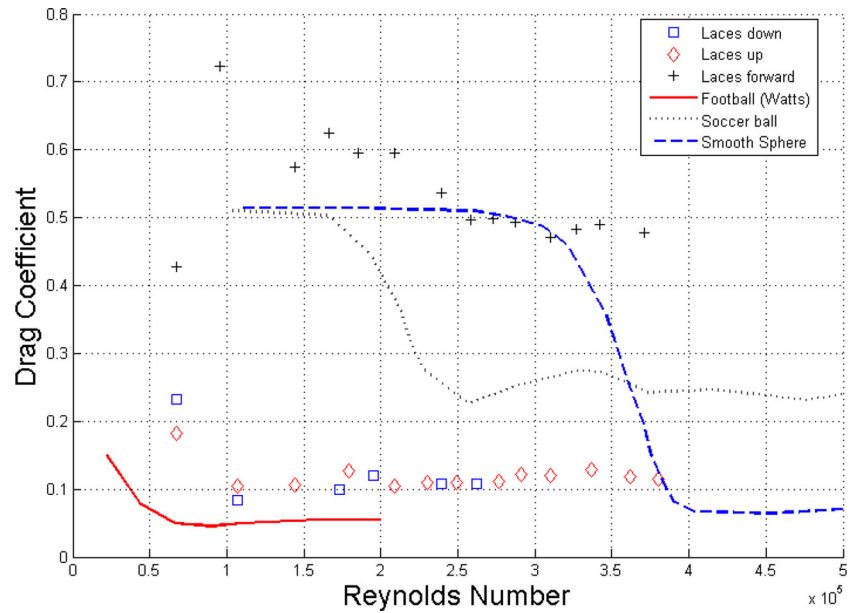


Fig. 3 Static drag coefficients

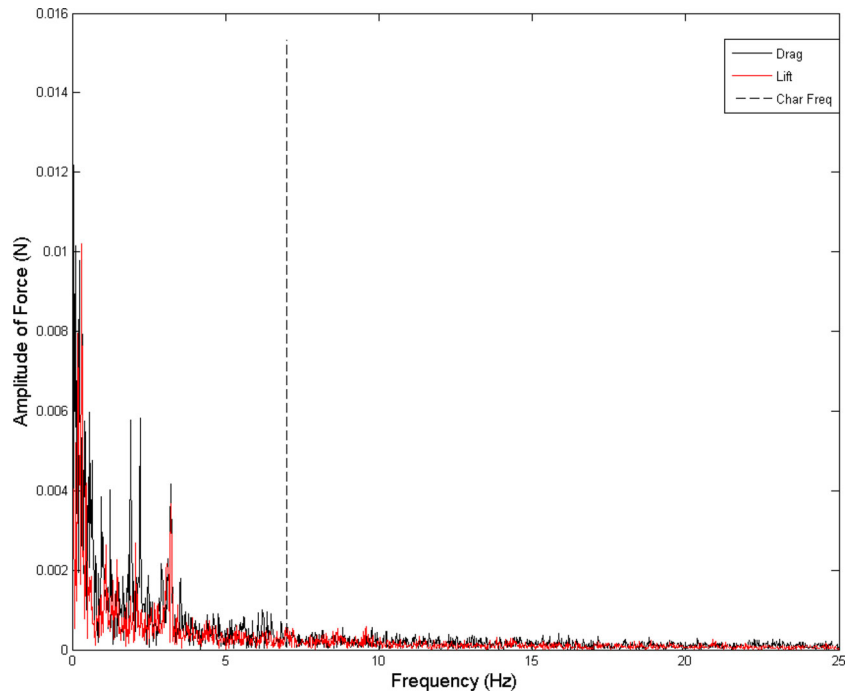


data from several other sources. The sharp drop in the drag is due to the boundary layer along the football transitioning from laminar to turbulent, at what is often called the critical Reynolds number. For rough objects, this critical Reynolds number is expected to be smaller than for the smooth sphere, and in fact this can be seen in Fig. 3. In both this study and the work of others, the critical Reynolds number for athletic balls of all types is significantly lower than that for a smooth sphere. Also noteworthy in Fig. 3 is the close agreement for drag coefficients between this study and that by Watts. This agreement serves as one level of validation of the methods in this study.

5 Lift and drag due to rotation

A number of datasets were taken at constant wind tunnel velocity with varying rotational velocities to determine the Magnus effect on the football. At rotational velocities approaching the high end in this study, even a very well-balanced ball appears to have some vibrations. To determine if these periodic oscillations in the ball and rig were due to aerodynamic effects or a mechanical imbalance, the ball was rotated over the full range of speeds with no wind velocity, and the time-resolved force data were recorded. The data acquisition system reading the wind tunnel's force

Fig. 4 Fourier transform of lift and drag forces at 210 RPM



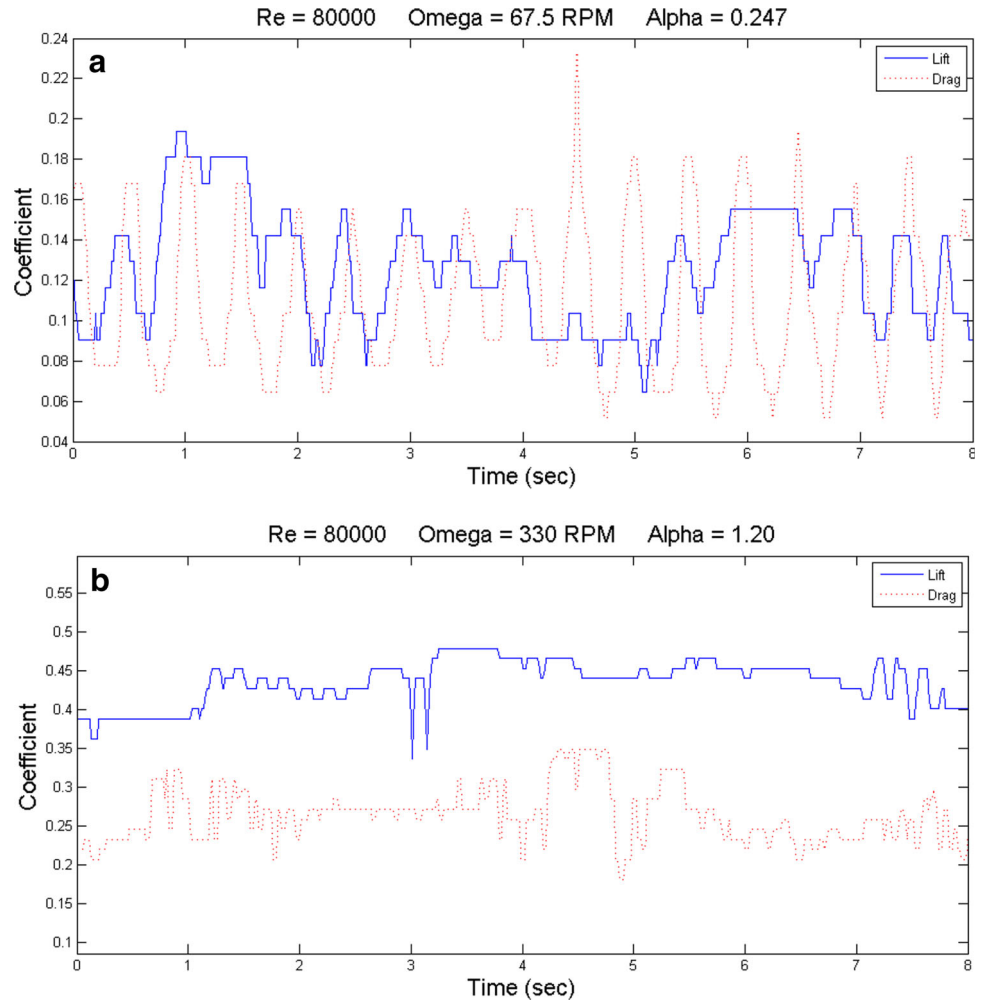
balance was capable of recording all forces at 15 ms intervals. Obvious periodic forces in both the lift and drag directions were evident. To determine the significance of these oscillations, the Fourier transform of the time-varying forces was performed with the resulting spectrum shown in Fig. 4 for a rotational speed of 210 RPM. The peak amplitude in both lift and drag force occurs at a frequency equal to the ball's rotation. The amplitude at this point is quite small, around 0.004 Newtons. When the spectrum for the same rotational velocity but with a wind speed of 20 m/s is compared, the peak amplitude occurs at a frequency of two times the ball's rotational speed and has a magnitude of nearly 90 times that seen in Fig. 4. This analysis shows that while the apparatus may oscillate during operation, the magnitude of the oscillations due to mechanical imbalance is insignificant when compared to the aerodynamically forced oscillations.

A number of researchers have attempted to predict the trajectory of rotating footballs by using average lift and drag coefficients measured when the ball is point forward or laces forward [13, 14]. In one study, the time-varying lift and drag were calculated based on the rotational aspect of the ball, but based on data measured without the ball rotating [15]. Figure 5 shows why this approach may lead to less accurate force calculations at higher values of the non-dimensional rotational velocity, α . The time-resolved lift and drag coefficients for two separate test cases, one at a low value and one at a high value of α , are shown in Fig. 5a, b. In Fig. 5a, the lift and drag coefficients vary a considerable amount as the aspect ratio of the ball with

regard to the flow field changes. The minimum drag coefficient is seen twice every revolution, when the ball is point forward. The maximum drag occurs 90 degrees out of phase with these minimums as the ball is either laces forward or laces back. A maximum lift coefficient occurs twice every revolution when the ball reaches an ideal angle of attack for the flow velocity. All of these occurrences are plainly evident in Fig. 5a, but not Fig. 5b.

Lift and drag coefficients as a function of the non-dimensional rotational velocity, α , were calculated after correcting for the effects of the bare rig, and are shown in Fig. 6a, b. Lift coefficients show a good positive Fig. 6. Dynamic lift and drag coefficients trend with an increase in α for most of the datasets as expected. For higher Reynolds numbers, the lift and drag coefficients showed an independence to Reynolds number. Based on the static testing and the results in Fig. 3, the critical Reynolds number for a football is expected to be around 2×10^5 . Below this Reynolds number, the lift and drag coefficients show more variability with respect to α , and, in the case of drag, do not show a general trend, but rather a peak and then fall off as α increases. This behavior can be attributed to the fact that the critical Reynolds number of an object is also influenced by the rotational speed. In the case for a Reynolds number of 1×10^5 , at a non-dimensional rotation velocity, α , below 0.4 the flow has not detached, but above that α the drag coefficient drops as the wake detaches from the rotating ball. This is an important insight because a large portion of the flight envelope of a kickoff may fall within this zone where the critical Reynolds number is affected by

Fig. 5 **a** Time-resolved lift and drag coefficients at 67.5 RPM.
b Time-resolved lift and drag coefficients at 330 RPM



the ball's rotational velocity. Above the critical Reynolds number, the flow is fully detached and the lift and drag coefficients are only a function of α . Most of the datasets in this study were taken near the critical Reynolds numbers based on the expected velocities and rotational speeds during a kickoff.

Another important insight that can be found in Fig. 6 is that the drag coefficient of the rotating football is not simply the average of the static drag coefficient with the laces forward and laces up. A number of researchers have attempted to predict the trajectory of a football by inferring the drag coefficient based on static measurements. Data from this study can be used to improve the accuracy of trajectory calculations.

6 Experimental uncertainty

The overall experimental uncertainty of the values for lift and drag coefficients was calculated by taking the root mean square of each parameter's uncertainty multiplied by

the lift or drag coefficient's derivative with respect to that parameter.

$$E_{\text{tot}} = \sqrt{\sum \left(\Delta E_1 \frac{\partial E_1}{\partial f} \right)^2 + \left(\Delta E_2 \frac{\partial E_2}{\partial f} \right)^2 + \dots} \quad (6)$$

For the case of the drag coefficient, the total experimental error would be

$$E_{\text{CD}} = \sqrt{\sum \left(\Delta F_d \frac{\partial C_D}{\partial F} \right)^2 + \left(\Delta \rho \frac{\partial C_D}{\partial \rho} \right)^2 + \left(\Delta A \frac{\partial C_D}{\partial A} \right)^2 + \left(\Delta V \frac{\partial C_D}{\partial V} \right)^2} \quad (7)$$

Table 2 summarizes the estimated uncertainty in each independent variable used in calculating the lift and drag coefficients, along with the maximum uncertainty of the coefficient based on Eq. 7. At the maximum fluid velocity used during this study, the maximum error expected in the coefficients was approximately 0.094, or between 13 and 55 % of the observed values of C_D and C_L . While seemingly high, this is the maximum possible error, and it is expected that the results are significantly more precise.

Fig. 6 Dynamic lift and drag coefficients

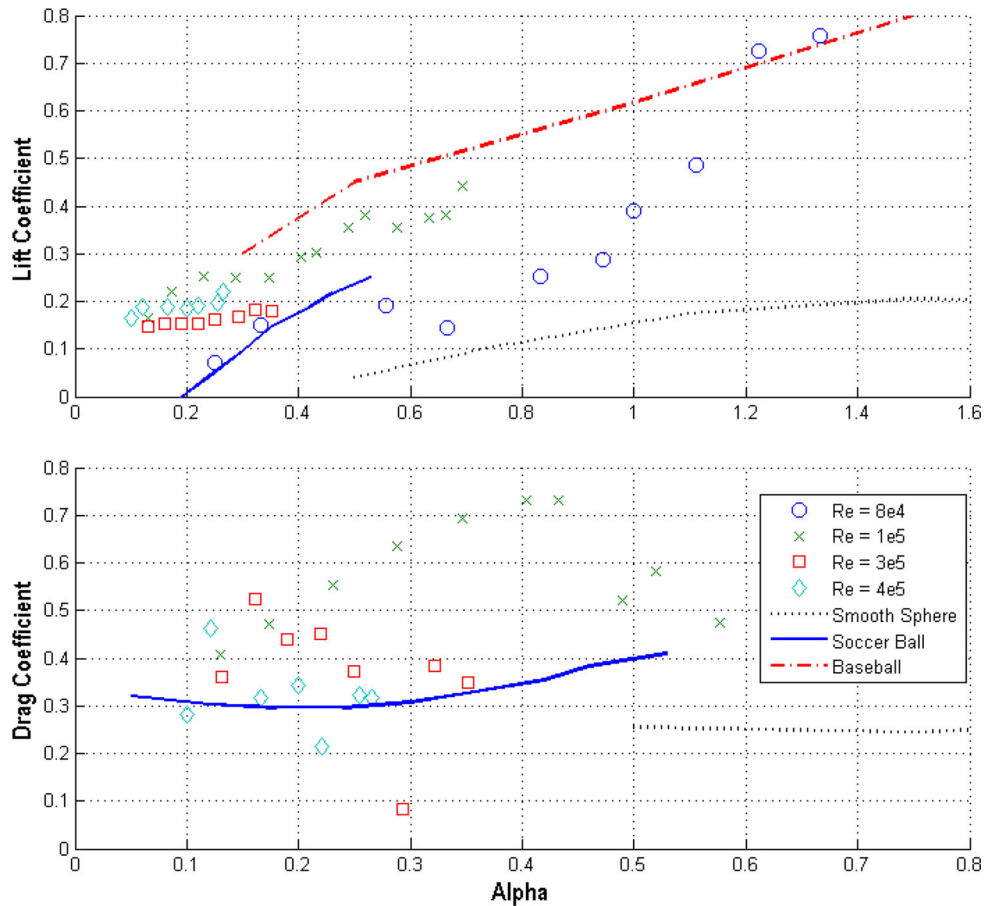


Table 2 Experimental sources of error and maximum total error

Variable	Value	Error
Lift force	Variable	5 N
Drag force	Variable	1.3 N
Air density	1.22 kg/m ³	1 %
Cross sectional area	0.0365 m ²	1 × 10 ⁻⁶
Velocity	5–25 m/s	1 %
Lift coefficient		0.093
Drag coefficient		0.094

7 Conclusions

The rotational velocity of an American football has a dramatic effect on its lift and drag. These forces dynamically change as the ball rotates, and simply using an average of the static results as has been done in previous studies is insufficient. By measuring the lift and drag coefficients over a wide range of rotational and fluid velocities, accurate predictions of end over end kick trajectories can be made through simple numerical integration. Further analysis can be performed to determine the optimal initial kick velocity, angle of trajectory, and

rotational velocity for a goal of either maximum range or flight time.

Acknowledgments The authors would like to acknowledge the support of the Mechanical Engineering Department at the Catholic University of America, the Aerospace Laboratory at the United States Naval Academy, and especially Ms. Louise Bectel and Mr. Don Smolley.

References

1. Newton I (1665) A letter of Mr. Isaac Newton containing his new theory about light and colors: sent by the author to the publisher from Cambridge, Feb 6 1672. *Philos Trans* 6:1665–1678
2. Magnus H (1852) On the deviation of projectiles; and on a remarkable phenomenon of rotating bodies. *Memoirs of the Royal Academy*, Berlin 1852. Eng translation in *Scientific Memoirs London*. p 210 Edited by Tyndall and Francis
3. Adair RK (1995) The physics of baseball. *Phys Today* 48(5):26–31
4. Briggs LJ (1959) Effect of spin and speed on the lateral deflection (curve) of a baseball: and the Magnus effect for smooth spheres. *Am J Phys* 27(8):589–596
5. Watts RG, Ferrer R (1987) The lateral force on a spinning sphere: aerodynamics of a curveball. *Am J Phys* 55:40–44
6. Asai T, Carre MJ, Akatuska T, Haake SJ (2002) The curve kick of a football I: impact with the foot. *Sports Eng* 5:183–192

7. Carre MJ, Asai T, Akatsuka T, Haake SJ (2002) The curve kick of a football II: flight through the air. *Sports Eng* 5:193–200
8. Asai T, Kamemoto K (2011) Flow structure of knuckling effect in footballs. *J Fluids Struct* 27:727–733
9. Alam F, Chowdhury H, Moria H, Fuss FK (2010) A comparative study of football aerodynamics. In: 8th conference of the international sports engineering association
10. Carre MJ, Goodwill SR, Haake SJ (2005) Understanding the effect of seams on the aerodynamics of an association football. *Proc J Mech Eng Sci Part C* 219:657–666
11. Kray T, Franke J, Frank W (2014) Magnus effect on a rotating soccer ball at high reynolds numbers. *J Wind Eng Ind Aerodyn* 124:46–53
12. Tanino K, Suito H (2009) Computational analysis for motions of rugby balls interacting with air flows. *Football Sci* 6:34–38
13. Alam F, Smith S, Chowdhury H, Moria H (2012) Aerodynamic drag measurements of American footballs. In: 9th Conference of the international sports engineering association
14. Watts RG, Moore G (2003) The drag force on an american football. *Am J Phys* 71:791–793
15. Lee WM, Mazzoleni AP, Zikry MA (2013) Aerodynamic effects on the accuracy of an endo-over-end kick of an american football. *Sports Eng* 16:99–113
16. Brancazio PJ (1987) Rigid-body dynamics of a football. *Am J Phys* 55:5
17. Hartschuh RD (2002) Physics of punting a football. Physics Department, the college of Wooster, Wooster
18. Fuss FK, Smith RM, Leali F (2013) Kick precision and spin rate in drop and torpedo punts. *Procedia Eng* 60:448–452
19. Goldstein S (1938) *Modern developments in fluid dynamics*. Oxford Press, London